A parent-school initiative to assess and predict air quality around a heavily trafficked school

Science of the Total Environment 861 (2023) 160587

Contents lists available at ScienceDirect

Science of the Total Environment

journal homepage: www.elsevier.com/locate/scitotenv

A parent-school initiative to assess and predict air quality around a heavily trafficked school

Prashant Kumar [a,b,*], Hamid Omidvarborna [a], Runming Yao [c,d]

[a] Global Centre for Clean Air Research (GCARE), School of Sustainability, Civil and Environmental Engineering, Faculty of Engineering and Physical Sciences, University of Surrey, Guildford GU2 7XH, Surrey, United Kingdom
[b] Institute for Sustainability, University of Surrey, Guildford GU2 7XH, Surrey, United Kingdom
[c] School of The Built Environment, University of Reading, RG6 6DF, United Kingdom
[d] Joint International Research Laboratory of Green Buildings and Built Environments (Ministry of Education), School of the Civil Engineering, Chongqing University, Chongqing 400045, China

HIGHLIGHTS

- Year-long monitoring, including during lockdown, was made at a school gate next to a busy road.
- Prophet Algorithm was used to predict NO_2 as a proxy to traffic emissions.
- Daily $PM_{2.5}$ levels increased by three-times the WHO limit right after the New Year.
- De-weathering of data showed no major changes, confirming existence of local emissions in all phases.
- Wind speed and temperature showed dominating effect on PM and gaseous pollutants, respectively.

GRAPHICAL ABSTRACT

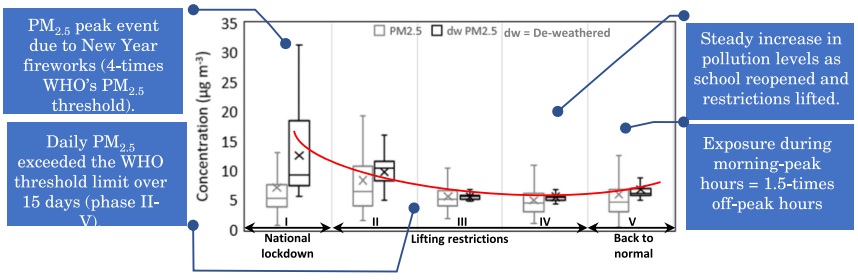

ARTICLE INFO

Editor: Pavlos Kassomenos

Keywords:
Air pollution
School gate
COVID-19 lockdown
Citizen science
De-weathering

ABSTRACT

Many primary schools in the UK are situated in close proximity to heavily-trafficked roads, yet long-term air pollution monitoring around such schools to establish factors affecting the variability of exposure is limited. We co-designed a study to monitor particulate matter in different size fractions (PM_1, $PM_{2.5}$, PM_{10}), gaseous pollutants (NO_2, O_3 and CO) and meteorological parameters (ambient temperature, relative humidity) over a period of one year. The period included phases of national COVID-19 lockdown and its subsequent easing and removal. Statistical analysis was used to assess the diurnal patterns, pollution hotspots and underlying factors driving changes. A pollution episode was observed early in January 2021, owing to new year celebration fireworks, when the daily average $PM_{2.5}$ was around three-times the World Health Organisation limit. $PM_{2.5}$ and NO_2 exceeded the threshold limits on 15 and 10 days, respectively, as the lockdown eased and the school reopened, despite the predominant wind direction often being away from the school towards the roads. The peak concentration levels for all pollutants occurred during morning drop-off hours; however, some weekends showed higher or comparable concentrations to those during weekdays.

Abbreviations: ARIMA, autoregressive integrated moving average; CO, carbon monoxide; COVID-19, SARS-CoV-2 disease; DEFRA, Department for Environment, Food & Rural Affairs; DfT, UK Department of Transportation; DW, de-weathered; GCARE, Global Centre for Clean Air Research; GLL, Guildford Living Lab; IQR, interquartile range; MAE, mean absolute error; N/A, not available; NO_2, nitrogen dioxide; O_3, ozone; PM, particulate matter; PM_1, PM with an aerodynamic diameter smaller than 1 μm; $PM_{2.5}$, PM with an aerodynamic diameter smaller than 2.5 μm; PM_{10}, PM with an aerodynamic diameter smaller than 10 μm; PR, parents/residents; Q, quarter; RH, relative humidity; RMSE, relative mean square error; RS, researchers; SARIMA, seasonal autoregressive integrated moving average; SARS-CoV-2, Severe Acute Respiratory Syndrome Coronavirus-2; SP, school personnel; ToNC, total particle number concentration; TRAP, traffic-related air pollution; WD, wind direction; WHO, World Health Organisation; WS, wind speed.

* Corresponding author at: Global Centre for Clean Air Research (GCARE), School of Sustainability, Civil and Environmental Engineering, Faculty of Engineering and Physical Sciences, University of Surrey, Guildford GU2 7XH, Surrey, United Kingdom.
E-mail addresses: P.Kumar@surrey.ac.uk Prashant.Kumar@cantab.net (P. Kumar).

http://dx.doi.org/10.1016/j.scitotenv.2022.160587
Received 11 September 2022; Received in revised form 19 November 2022; Accepted 26 November 2022
Available online 5 December 2022

The strong disproportional Pearson correlation between CO and temperature demonstrated the possible contribution of local sources through biomass burning. The impact of lifting restrictions after removing the weather impact showed that the average pollution levels were low in the beginning and increased by up to 22.7 % and 4.2 % for $PM_{2.5}$ and NO_2, respectively, with complete easing of lockdown. The Prophet algorithm was implemented to develop a prediction model using an NO_2 dataset that performed moderately (R^2, 0.48) for a new monthly dataset. This study was able to build a local air pollution database at a school gate, which enabled an understanding of the air pollution variability across the year and allowed evidence-based mitigation strategies to be devised.

1. Introduction

The UK road transport sector accounts for a significant proportion of traffic-related air pollution (TRAP) such as $PM_{2.5}$ (particulate matter with an aerodynamic diameter smaller than 2.5 μm), CO (carbon monoxide) and NO_2 (nitrogen dioxide) emissions (NAEI, 2021). In the UK, many schools are located adjacent to busy roads for better accessibility (Dowler and Howard, 2017; Osborne et al., 2021a, 2021b). Furthermore, the use of personal cars for school journeys in England has doubled over the past two decades accounting for as many as 1 in 4 cars on the road during morning peak hours (Perscom, 2018). Hence, infiltration of exhaust emissions from these roads or idling vehicles during drop-off/pick-up hours may lead to elevated air pollution exposure in young children (Kumar et al., 2020a, 2020b). Consequently, children are more likely to suffer from short- and long-term health conditions (Brumberg et al., 2021; Shier et al., 2019), including asthma, bronchitis and stunting of their incomplete lung development as well as exhibiting higher breathing rates and low-breathing height as compared to adults (Kumar et al., 2020a, 2020b; Sharma and Kumar, 2018). Reducing car usage, wherever possible, and prompting active travel can positively impact the reduction of fresh exhaust emissions and children's exposure to them.

The Severe Acute Respiratory Syndrome Coronavirus-2 (SARS-CoV-2), which is the responsible agent of SARS-CoV-2 disease (COVID-19), reached the UK in early 2020. As a result, the UK government announced and encouraged the population to stay at home, commonly known as 'lockdown', on 23 March 2020 (GOV.UK, 2020) and brought into force mandatory restrictions on non-essential travel across the UK (PHE, 2020). These restrictions limited mobility and on-road activities to essential services/travel causing a significant reduction in on-road vehicles and subsequently TRAP (Gkatzelis et al., 2021; Kumar et al., 2020c; Lee et al., 2020; Venter et al., 2020). However, after the step-by-step easing of restrictions, which led to schools reopening in the UK on 08 March 2021, parental concerns related to children's exposure to elevated TRAP around schools became valid again.

Due to the advances in low-cost sensing technologies for air quality monitoring in recent years, multi-sensor units have been introduced to the market and are widely utilised (Kumar et al., 2015; Omidvarborna et al., 2021; Rai et al., 2017). Real-time air quality monitoring by schools can help them to understand the diurnal patterns of air pollution and devise appropriate mitigation plans to limit school children's exposure. Therefore, we researchers, parents and the school in this study, co-designed a study to continuously monitor air pollution during and beyond the lockdown periods. The de-weather algorithm was used to decouple the weather effects from the monitored data. We applied simple machine learning forecasting models to predict the concentrations and identify the forces driving temporal changes in local air quality. Although there are conventional, but complicated, air quality forecasting models (Deters et al., 2017; Xi et al., 2015) and machine learning forecasting models (Deters et al., 2017; Fuller et al., 2002; Li et al., 2015), we utilised a versatile machine-learning-based model, the Prophet algorithm, which is not complex to operate and is independent of meteorological factors (Taylor and Letham, 2018). The specific objectives were to (i) measure air pollution concentrations during different phases of lockdown easing and evaluate the extent to which these changes affected the air quality at a school gate; (ii) understand the influence of meteorological factors on monitored air quality data after decoupling their effects, (iii) apply a simple but effective machine-learning model to predict air pollution concentrations and hotspots; and (iv) facilitate discussion among researchers, parents and school staff to design actions that could raise awareness and reduce children's exposure to air pollution.

2. Materials and methods

2.1. Study design

Guildford Living Lab (GLL), run by researchers from the University of Surrey's Global Centre for Clean Air Research (GCARE), is a platform involving researchers, local communities and stakeholders to co-create and co-design sustainable and evidence-based solutions to tackle air pollution and to raise awareness about air pollution and climate change through citizen science activities (GLL, 2021; Mahajan et al., 2020; Omidvarborna et al., 2020). Air quality concerns are brought in to the GLL by community members, environmental groups or the public through workshops, webinars or public engagement activities via social media and physical events such as Car Free Day (CFD, 2021). This allows diverse stakeholders to interact, discuss and co-design studies on issues related to local air quality and climate change.

The concepts of inclusion, collaboration and reciprocation were included in this co-creation citizen science activity (Mahajan et al., 2020; Omidvarborna et al., 2020). Inclusion involved the parents of primary school children and nearby residents (PR) contributing to the scientific work in conversations with school personnel (SP) and the researchers (RS) of the GLL to build an understanding of air pollution levels and their causes. The collaboration was established among PR, SP and RS in mid-2020 through a series of virtual meetings to co-design the scientific objectives of the study. This step involved site selection (SP and RS), installation of equipment (SP and RS), overseeing the operation and safety of equipment (SP), data collection and analysis (RS), writing reports and the interpretation of results (RS). During this process, a co-implementation plan of the strategy and the responsibilities of all three groups for the collaborative steps outlined above was also agreed upon. During the monitoring period, the collected data were analysed monthly and interpreted by the RS and then discussed with others (PR and SP) during monthly meetings in which all parties addressed the air pollution events, concentration trends, sources and possible mitigation scenarios. For example, apart from considering natural green barriers to mitigate air pollution (Abhijith et al., 2017; Abhijith and Kumar, 2019), the use of aesthetically-pleasing solid messaging boards that can include educational messages (adopted from the general and targeted recommendations in Kumar et al., 2020b) was also considered. These messaging boards can be placed above the green barriers along school boundaries to limit the ingress of new exhaust emissions to school premises from adjacent busy roads. An example of a co-designed barrier through this citizen science activity is shown in Fig. S1. The last step, called reciprocation, involves the dissemination, engagement and conversion of complex science into simple messaging (PR, SP and RS) in the shape of storytelling (see Fig. 1).

2.2. Site description

Fig. 2 shows the location of the primary school in the town centre of Guildford, UK. The school is situated near heavily-trafficked roads 1 (East-West direction) and 2 (North-South direction). Guildford is one of

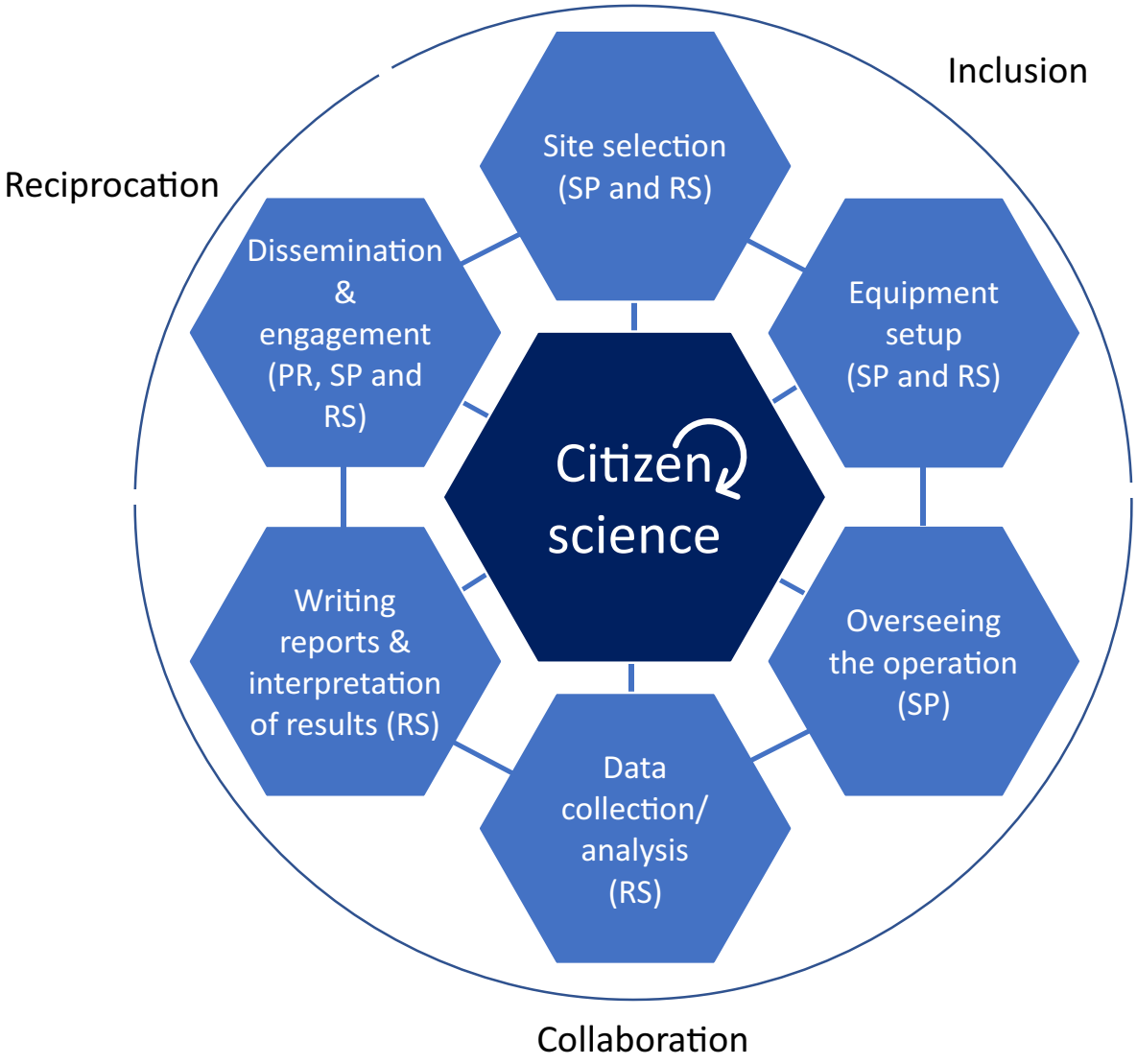

Fig. 1. The conceptual framework of the citizen science activity at the school site includes the contribution of each partner - RS, SP and PRa. The dissemination and post-exploitation steps informally start from the beginning of any citizen science activity. This means that the development of public engagement and raising public awareness require continuous involvement and dissemination across the study period.

the most populous towns in the County of Surrey in England with a population of around 143,600 in 2021 (Office for National Statistics, 2021). As reported by the UK Department for Transport (DfT), four major roads pass through Guildford (DfT, 2012), which attract about 43,746 to 96,135 vehicles per day to this area (Surrey-i, 2015). This is subject to increase due to Guildford residents' high personal car ownership rate (72%) (Al-Dabbous and Kumar, 2014) which makes cars the most preferred mode of transport (~97 %). Thus, traffic is the primary emission source given the lack of local industrial or thermal power plants (Surrey-i, 2015). As the roads around the school connect Guildford town centre to nearby areas, queues of cars are expected during the peak hours. For example, the routes to the east side of Guildford via road 1, to Woking via road 2 and vice versa to the town centre are highly used on a daily basis. In addition to passenger cars, vans, lorries and other diesel-powered vehicles use these roads to provide support and deliver goods to local shops/residents.

To capture air pollution from both roads, the monitoring unit was installed at the breathing zone height of about 1.8 m, where the unit can operate safely. The unit was 20 m away from road 1, where a break-type wall (approximate height = 1.8 m) and partial green infrastructure (see the image directed by purple lines) were located (Fig. 2). The distance of the unit from road 2 was around 15 m, where a porous wooden fence was in place (see the image directed by turquoise blue lines). The onsite wind speed (WS) and wind direction (WD) measurements were unavailable. However, such data are essential information for de-weathering purposes. Therefore, meteorological data were obtained from the closest meteorological station in Wisley (5062E 1579 N) located about 11 km to the North-East of the sampling site. This station is run by the Met Office National Meteorological Archive and its data has been successfully used in previous Guildford-based studies (e.g. Goel and Kumar, 2016; Kumar et al., 2022). The meteorological data have proven to be valid for Guildford (R^2, 0.89), as reported in a recent modelling study by Tiwari et al. (2021).

The colour-coded WD illustrates the number of pollutants that could be transferred into the school with the red colour representing the highest exposure from the vehicular emissions associated with WD and the green colour showing the lowest possible exposure. As shown in Fig. 2, wind towards the school covering the first quarter (Q1 represented by the red colour covering 0° to 90°), wind from the school covering the third quarter (Q3 represented by the green colour covering 180° to 270°), and wind parallel to Road 1 (Q2 covering 90° to 180°) and Road 2 (Q4 covering 270° to 360°) coloured yellow were defined accordingly.

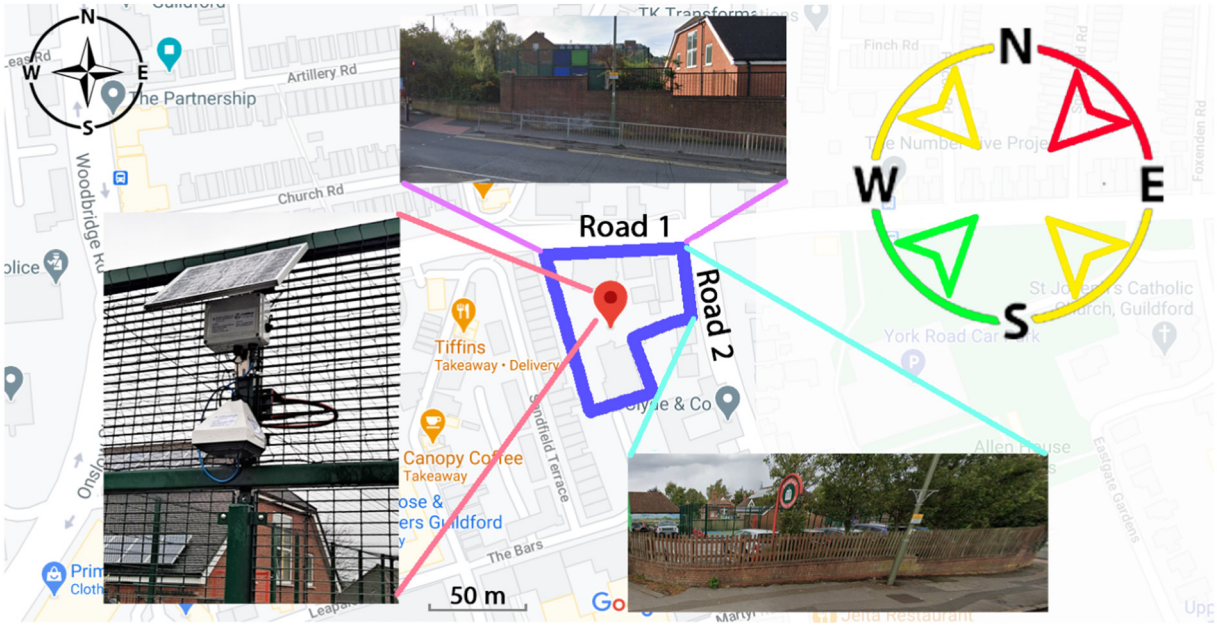

Fig. 2. The location of the school (dark blue enclosure) and AQMesh (red location sign in the middle of the school) concerning roads. The WDs from/to the school are shown in red, green, and yellow colours, respectively, as described in Section 2.2.

2.3. Instrumentation and data collection

A solar-powered and rechargeable battery-operated AQMesh pod (Environmental Instruments Ltd., UK) was utilised to measure particles of different size fractions (PM_1, $PM_{2.5}$ and PM_{10} μg m^{-3}), NO_2 (μg m^{-3}), CO (μg m^{-3}), ozone (O_3; μg m^{-3}), temperature (accuracy of 2 °C), and RH (accuracy of 5 %). The NO_2 sensor is designed to reject O_3 and thus minimise O_3–NO_2 cross-sensitivity issues. The raw data can be accessed by a secure login for different time intervals from 15 min to 24 h. The versions of the AQMesh platform for the Gas Protocol and the Particle Protocol were 5.1 and 3.0, respectively. The recorded data from the pod were uploaded via cellular communication to a cloud database held by the provider.

2.4. Data collection

The UK government roadmap for ending all COVID-19 restrictions involved multiple stages in precisely five phases in total, in the year 2021 (Fig. 3a). Since the major source of air pollutants around the school is from nearby roads, we further elaborated on these five phases in Table 1. Phase II/III (previous school year 2020–21 after reopening) and phase V

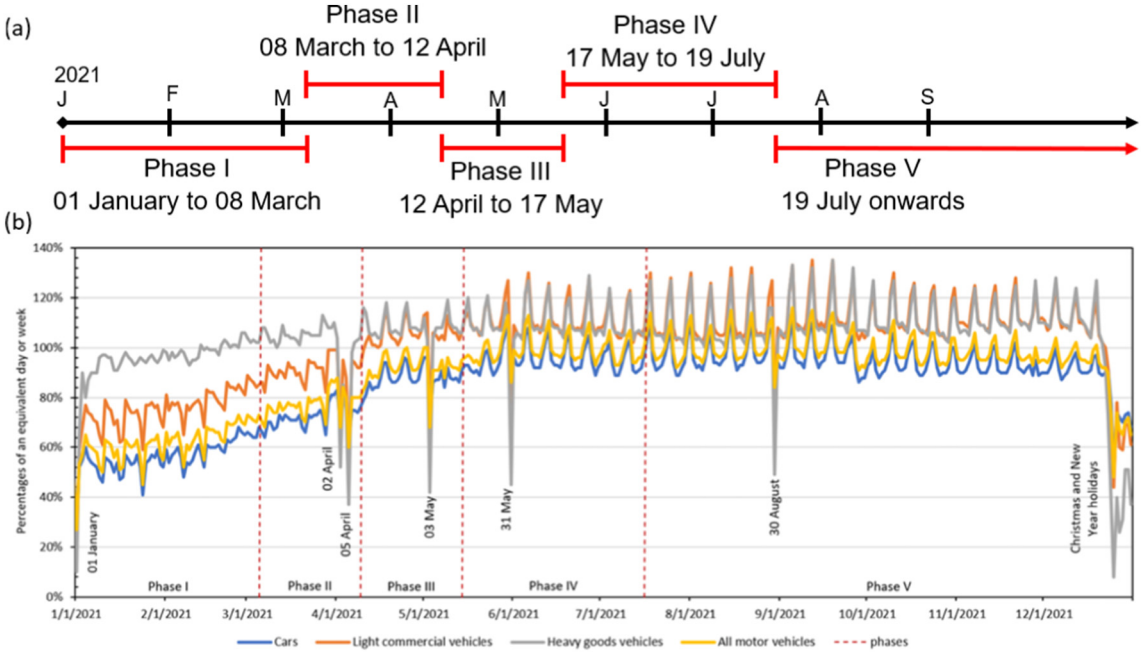

Fig. 3. (a) Easing restriction dates by the UK government during the year 2021. (b) The UK DfT statistics on domestic transport use during the Covid-19 pandemic (DfT, 2021). The sudden reductions in domestic transport use are linked to public holidays. The school considered in this study embraced remote classes until 08 March 2021 and later resumed normal operation to conclude the 2020–21 academic year.

Table 1
Easing restrictions details as per the UK government plan and statements by the Prime Minister's Office (GOV.UK, 2021).

Phase	Duration (from 2021)	Description
I	Up to 08 March	Stringent lockdown measures in the UK from the beginning of January 2021, which included: • Stay at home with limited exceptions. • School closures. • Closure of non-essential shops and services.
II	Up to 12 April	Schools reopened - but other measures remaining in place.
III	Up to 17 May	Opening of non-essential retailers and hospitality venues serving outside.
IV	Up to 19 July	Allowing indoor hospitality and larger outdoor gatherings like some sporting events with spectators.
V	19 July onwards	Getting back to the normal situation with minor restrictions. 30 November onwards: new measures to respond to the emergence of the Omicron variant come into force at 4 am - compulsory face coverings in shops and on public transport.

(ongoing school year 2021–22) represent the time when school children have been exposed to pollutants as compared to phase I (school closure and operating online due to the UK national lockdown) and phase IV (school closure, summertime).

Moving through these phases revealed variations in the number of on-road vehicles and higher vehicular emissions irrespective of meteorological and local conditions. As shown in Fig. 3b, the report released by the DfT reveals that domestic car usage started to increase when lockdown measures were eased. For example, from the school reopening date (08 March 2021, beginning of phase II) and the week commencing mid-May (17 May 2021, beginning of phase IV) onwards (Table 1), the number of domestic vehicles increased towards the maximum level and remained constant across the UK. Since there was no local transport use in place during the periods, we assumed a similar increase in the number of on-road vehicles around the school to that shown by DfT statistics.

The pod is adjusted to deliver 15-min averaged data. We used the standard hourly data averaging merged with the meteorological data to reduce random noise (Section 2.5). In total, 8760 data entries per hour per monitored variable and meteorological data were obtained during the study domain covering a full calendar year from January 2021 until the end of December 2021.

2.5. Data analysis

Considering the situations, the final dataset was assessed for the different phases of lockdown and its subsequent easing and removal during school hours (08:00 to 16:00 h), non-school hours (<08:00 and >16:00 h) and weekends (00:00 to 23:00) as seen in Table S2. To explore the impact of WD on air pollution, we analysed the dominant winds in three main directions as described using different colours in Section 2.2 (see Fig. 2). Following standard practice, a WS < 0.5 m s^{-1} was used to represent calm wind conditions.

We assessed the role of weather on the observed data using the deweather code in the R package for removing meteorological variation from the air quality data (Carslaw, 2020; Grange and Carslaw, 2019). The de-weathering code operates based on an ensemble of decision trees to de-trend the cleaned dataset and remove the influence of meteorological variables. The de-weather approach is based on a non-parametric model using boosted regression trees to model the relationship between pollutants and the explanatory variables (Carslaw and Taylor, 2009). This exercise allowed us to assess the extent to which changes in ambient pollutant concentrations were attributed to changes in emission levels during the different phases of lockdown and beyond (Grange and Carslaw, 2019). Apart from meteorological factors, time variables such as 'hour', 'weekday', and 'trend' were selected as proxies for the determination of diurnal variations in emissions (Carslaw, 2020). De-weathered data for pollutants was annotated as "*dw*". All the codes for in-depth analysis of the plots, for removing the influence of meteorological events and for statistical analysis were achieved with the help of 'Openair' open-source software (Carslaw and Ropkins, 2012) in RStudio (version 1.1.456) developed under the R project (R Development Core Team, 2013) for the statistical computation of air pollution data.

2.6. Quality control and assurance

Past studies, e.g. monitoring at a railway station in Birmingham, UK (Hickman et al., 2018) and another one in kindergartens in Oslo, Norway (Castell et al., 2018), have shown the reliable performance of AQMesh pods in monitoring ambient air quality. Here, we summarised the reported performance of AQMesh units in comparison with references in Table S1, where ambient air quality was in focus. In this study, we followed the procedure proposed by the manufacturer (Environmental Instruments Ltd., Stratford-upon-Avon). We deployed a factory-calibrated pod at the school site. Secondly, the pod was left in operation for up to two weeks for stabilisation before initiating the campaign. Thirdly, a proprietary algorithm was implemented to post-process the data recorded by the sensors to resolve the effect of temperature/RH as well as cross-interferences. The data points obtained from the pod with a valid status tag were retained and all the negative, not available (N/A) and 'out-of-spec' values were removed following the manufacturer's specifications. Lastly, the collected hourly dataset was combined with the cleaned meteorological data for applying outlier and/or anomaly detection techniques using the previously developed sensor toolbox (Mahajan and Kumar, 2019).

2.7. Model description

We used an R-based forecasting model, the Prophet algorithm, which was supported by the history of temporal relationships during the past 12 months. This algorithm implements machine learning fitting and time series decomposition methods (Kakoullis et al., 2021) to successfully return a high accuracy time series forecast to predict future air pollution events (Nath et al., 2021; Sadhasivam et al., 2021; Topping et al., 2020; Ye, 2019). The Prophet algorithm is a robust model for outliers, missing data and dramatic/unexpected changes in time series events (Taylor and Letham, 2018). Even in the presence of numerous outliers or missing values (Ye, 2019), the Prophet algorithm requires less time for training and conformity with known predictive models such as autoregressive integrated moving average (ARIMA) and seasonal autoregressive integrated moving average (SARIMA), which make it our preferred candidate as a forecasting model (Ye, 2019; Samal et al., 2019).

We considered the hourly concentration of NO_2 for this modelling since it serves as a good proxy for vehicular emissions. The implementation of the algorithm was done in R and used to forecast the level of NO_2 in the first month of the year 2022. Theoretically, the model can forecast longer periods; however, forecasting with better precision using the most recent data is preferred. To validate the performance of the model in forecasting air quality around the school, the model was evaluated against the observations using a set of statistical parameters.

3. Results and discussion

3.1. Impact of lockdown and lockdown eases

To understand school children's exposure to air pollution during different phases of lockdown and post-lockdown measures, we divided all the data into school hours (0800 to 1600 h), non-school hours (<0800 to >1600 h), and weekends. In the subsequent sections, we will pay most attention to school hours, as the school children are mainly exposed to TRAP during their presence at the school. It is worth noting that the school hours also include the school children drop-off time in the morning and the evening pick-up. Non-school hours are discussed as the second priority to support the study topic in Section S2 (Figs. S2–S10).

	Phase I	Phase II	Phase III	Phase IV	Phase V
PM_1	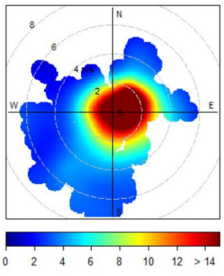	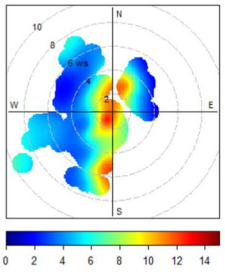	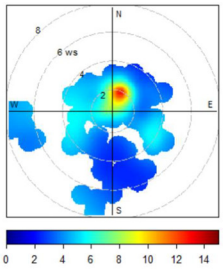	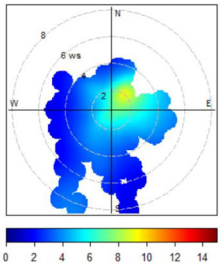	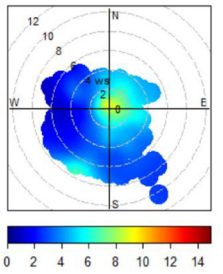
$PM_{2.5}$	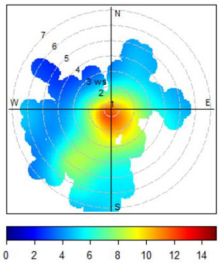	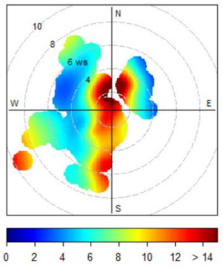	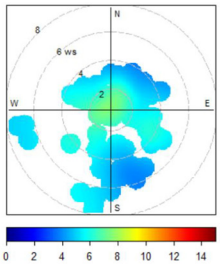	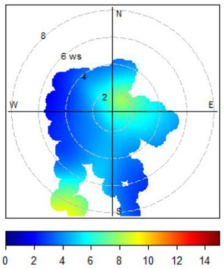	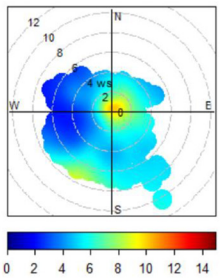
PM_{10}	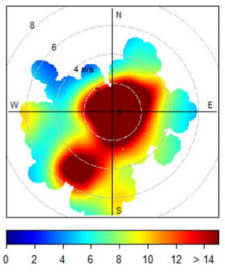	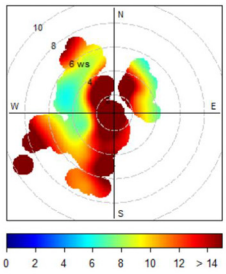	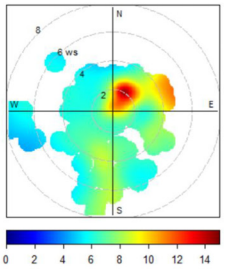	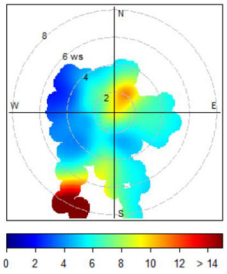	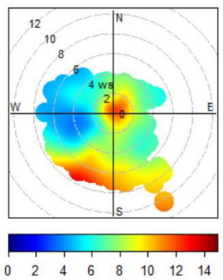
NO_2	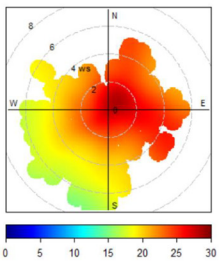	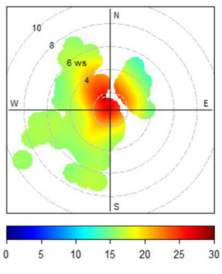	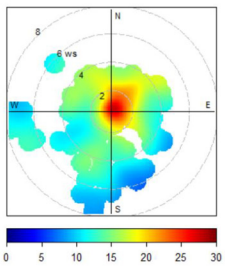	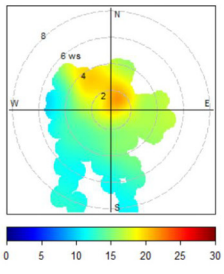	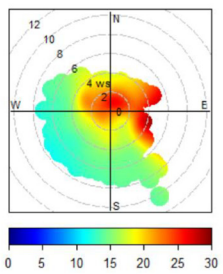
O_3	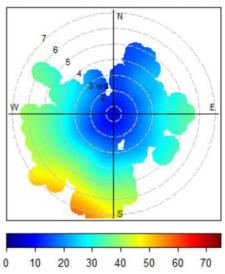	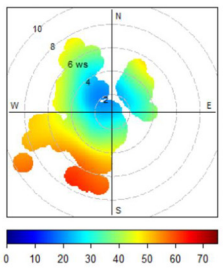	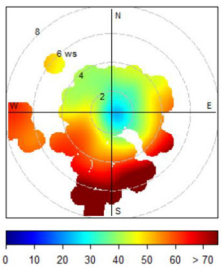	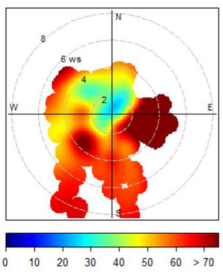	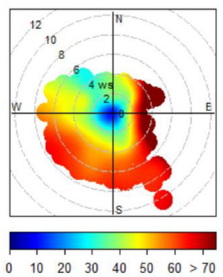
CO	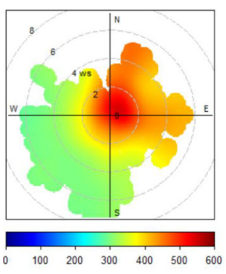	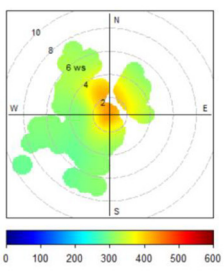	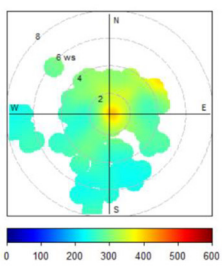	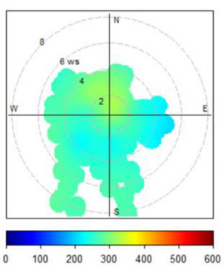	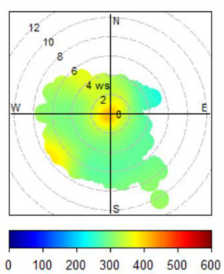

3.1.1. PM size fractions

During phase I, when the school was closed due to national lockdown, the diurnal variation of $PM_{2.5}$ and PM_{10} showed a noticeable change, especially during morning hours as compared to other times of the day (Fig. S3). The exposure to PM during morning peak hours is up to 1.5-times higher than daily off-peak hours. This is due to the traffic associated with essential workers' schedules. However, the peak traffic in the evening was spread out as the working time schedules might vary. This trend remained in place in other phases not only because of essential workers but also as a result of school reopening.

During phase I (Fig. S2 and Table 1), the dominant WD was from the school to traffic (Q3 followed by Q2 and Q1). Hence, a noticeable dispersion was expected (3.16 m s^{-1}; 0.7 % calm) due to a high mean WS and less calm conditions compared with non-school hours (2.81 m s^{-1}; 0.9 % calm) and weekends (2.40 m s^{-1}; 1.9 % calm). However, as shown in Fig. 4, a significant variation in PM covering all size fractions was observed in phase I. The first possible reason would be new-year fireworks activities, when the daily average PM concentration reached 27, 40 and 46 μg m^{-3} levels for PM_1, $PM_{2.5}$ and PM_{10}, respectively. Additionally, the presence of an unexpected source emitter very near to the pod around 07 January 2021 elevated the daily average concentrations of PM_1, $PM_{2.5}$ and PM_{10} by 11-, 13-, and 18-times with respect to the baseline concentration on preceding days. On this day, the absolute concentration values for PM_1, $PM_{2.5}$ and PM_{10} were 29, 54, and 116 μg m^{-3}, respectively. These extreme events happened during weather conditions when WS was <2 ms^{-1} (Fig. S2). All these activities are also evident in the representative $PM_{2.5}$ calendar plot (Fig. S5), when the $PM_{2.5}$ threshold is set at 15 μg m^{-3} following the recent World Health Organisation guideline (WHO, 2021). Likewise, there were two days in February 2021 (01 and 22) and four consecutive days in March 2021 (01–04) when the daily levels exceeded the WHO limits. Exposure to such PM levels could easily put school children into unhealthy situations since concentration values were within the moderate and very high bands as defined by the UK Air index (UK Air, 2021). All these events happened during phase I when the school was not in operation. These events have increased the exposure level of local residents to PM in different size fractions. Hence, there is a need for a warning tool to minimise outdoor activities and propose mitigation actions to reduce the ingress of polluted ambient air into classrooms.

Phase II represents the school reopening period when a higher concentration of PM was expected. As is evident in Fig. 4, the concentration of PM notably increased at the junction (Q1 segment) and along Road 2 (North to South direction), where the distance of the pod from the road is minimum and the school has no solid barrier (Fig. 2). The traffic associated with school reopening (phase II) has reflected its impact in elevating the daily $PM_{2.5}$ concentrations in March as compared to earlier days. In addition to the school opening day, the daily $PM_{2.5}$ concentration level on four school days in this phase did not meet the recent WHO threshold of 15 μg m^{-3} (Fig. S5). This indicated the high exposure level during the school reopening which could impact the children's daily exposure. The air pollution level in the school could have been even greater if the dominant WD was not from Q3 (Fig. S2).

Polar plots for phase III also reflected impacts from the junction/road emissions (Fig. 4). As compared to phase II, the PM concentrations were lower in phases III and IV (Figs. S4 and S5); however, the average concentrations showed a slight increase starting from phase III as described later (Section 3.2). During the summer break and school closure time, i.e. the last few weeks of phase IV and the first few weeks of phase V, the favourable WD (Fig. S2) and no drop-off/pick-up activity reduced the daily concentrations of PM as represented by Figs. 4 and S5. For example, as shown in Fig. S5, there was no day in August 2021 with a daily $PM_{2.5}$ concentration >8 μg m^{-3}.

Phase V can be officially called the normal situation when all the restrictions are lifted and a stable flow of on-road vehicles is established (Fig. 3b). During this phase, school children attended indoor classes with open windows and/or activities inside the premises to avoid the possible transmission of infectious diseases due to lack of proper ventilation. However, leaving windows open or having outdoor activities could expose them to the TRAP from adjacent roads (Kumar et al., 2021). The polar plot for phase V illustrates the hourly PM concentration build-up in the school environment under low-WS conditions (Figs. 4, S2) as compared to summertime (i.e. phase IV). As shown in the calendar plot (Fig. S5) and later described in Section 3.2, the median PM concentration for all size ranges increased to its maximum level since the beginning of phase III. For example, the number of days with a daily $PM_{2.5}$ concentration greater than the WHO threshold limit increased to 8 weekdays from September onwards. Therefore, leaving windows open or having activities outdoors is not recommended. An alert can be achieved by deploying an alarm indicator that is capable of monitoring school-site ambient air quality and feeding the data into a prediction model to forecast air pollution levels (see Section 3.3).

3.1.2. NO_2 and O_3

Monitoring NO_2 concentration as a traffic indicator could be of great importance in the school environment (GOV.UK, 2018), where diesel-based lorries/vans are responsible for delivering goods and services to local shops/residents. NO_2 is sourced mainly from the transportation sector, especially diesel engine emissions, and is a proxy for vehicular emissions. As seen in Fig. 4, the NO_2 and $PM_{2.5}$ plots follow a very similar pattern with moderate positive correlations (Fig. S9). The higher concentrations of NO_2 are detected when the wind blows from the direction of intersections and roads towards the school in all phases (Q1, Q2, and Q4; see the surge of NO_2 in Fig. 4), while a WD from the school (Q3) brought in minimal NO_2.

The hour of the day shows the diurnal variation in emissions in which the NO_2 is at its highest level during school hours (see Fig. S3) and remains high throughout the day until evening with a strong correlation with daily commutes (Ragettli et al., 2015). The NO_2 level was usually low at weekends (Figs. 4 and S6) compared to weekdays due to reduced flows of diesel vehicles (see NO_2 Calendar Plot in Fig. S8). After the school reopened in March 2021, NO_2 levels crossed the WHO threshold (25 μg m^{-3}) during 10 weekdays.

As shown in Figs. 4, S6 and S7, the relationships between the secondary pollutants NO_2 and tropospheric O_3 and meteorological variables are in keeping with those expected based on knowledge of the physical conversion process involved (Monks et al., 2015). The reciprocal relationship between NO_2 and O_3 was evidenced by strong negative correlations $r = -63$, -78 and -89 during the first three phases (Fig. S9), while the correlations became weak in other phases. The increase in O_3 levels started in mid-March, most likely driven by warmer weather through photochemical reactions and lockdown easing as the potential sources (Mahato et al., 2020). Furthermore, a higher WS facilitates dilution and atmospheric mixing, which elevates the formation of O_3 through better mixing and/or physical interactions (Fig. S7). Although the local council is monitoring NO_2 levels across Guilford, but not around the school, using diffusion tubes, our results indicate that a specific site for NO_2 sampling near the school should be considered.

3.1.3. CO

CO arises from the incomplete combustion of fossil fuels and biomass (e.g. wood) in vehicle engines and many household appliances e.g. boilers,

Fig. 4. Representative hourly polar plots for all pollutants during different phases of monitoring and school hours (weekdays from 0800 to 1600). For clarification, the centre of the plots is assumed to be the placement of the monitoring station. Simply, the West to East line can represent Road 1, while the North-South line can be counted as Road 2. The circular format of each diagram shows the directions (refer to Q1 to Q4 WD segments as discussed in Section 2.1) from which the winds blew and the colour in each segment shows the concentration of pollutants. The colour bars underneath the plot represent concentration levels in μg m^{-3}.

central heating systems, gas fires, water heaters, cookers and open fires (GOV.UK, 2018). Fig. 4 shows variations in CO concentration in all phases even after easing restrictions as compared to other pollutants, with minimal variations being observed during non-school hours and weekends (Fig. S10). Although there is a good correlation between CO and $PM_{2.5}$/NO_2, the strong disproportional Pearson correlation between CO and ambient temperature in phases I to V (−72, −70, −70, −51 and −51, respectively; Fig. S10) could suggest that nearby households play a role. Although the measured CO levels were below the Department for Environment, Food & Rural Affairs (DEFRA) guideline (10,000 μg m^{-3} as an 8-h average), a recent multi-country study (337 cities avoiding potential publication bias) by Chen et al. (2021) concluded that daily exposure to CO concentrations of >600 μg m^{-3} is significantly associated with mortality risk estimates. Hence, a detailed source apportionment analysis supported by additional monitoring is required to track the contribution of each factor in the school environment.

3.2. Weather impact

The *dw* approach is used to remove the influence of weather (meteorology) and detect the timings of discrete changes in PM_1, $PM_{2.5}$, PM_{10}, NO_2, O_3, and CO time series (Carslaw, 2020; Grange and Carslaw, 2019). Although complex interactions and nonlinearity effects among air pollutants have been involved, the statistical model illustrated strong correlations with the *dw* model ($0.79 \leq r \leq 0.92$) to reproduce observations as shown in Table S3 (Emery et al., 2017; Henneman et al., 2017). Using the *dw* model, we explored the relative importance and levels of the explanatory variables scaled as percentages for specific pollutants (Fig. 5) in order to understand the relationship between each pollutant and the covariates used in the model while holding the value of other covariates at their mean level (Carslaw and Taylor, 2009; Friedman, 2001).

As shown in Fig. 5, the time evolution (trend) was the most important variable in the PM explanation, while temperature mainly controlled the predicted values for gaseous pollutants. Among the other meteorological factors, WS (plume dispersion) had a larger impact on both PM and gaseous pollutants compared with WD. RH can have an appreciable impact on the growth of PM due to hygroscopic effects. However, a correction for the hygroscopic growth of particles is usually required when RH > 85 % (Crilley et al., 2018; Jayaratne et al., 2018). Although average RH was slightly outside the range on a few occasions during school hours (SI Table S2), a built-in filter (AQMesh proprietary algorithm and PM processing tool (v3.0)) minimised the effects on hygroscopic particles. The diurnal hourly pattern in the model showed insignificant impacts on PM and medium impacts on gaseous pollutants.

Observed concentration (dashed grey), noiseless *dw* (solid black) and their associated variations are shown in Figs. 6 and 7, respectively, where the phases are separated by vertical lines. The temporal variations of observed concentrations at the school site (Fig. 6) did not show a smooth trend because of concentration spikes during pollution events. The O_3 and CO concentrations varied more markedly after phase I, because their variations are temperature dependent (Fig. 5). The *dw* trends in Fig. 6 show that there were no distinguishable sharp increases or sudden drops from one phase to another, which indicated a more gradual change in *dw* concentrations (see Fig. 7). For example, the *dw* plots for PM in different size fractions showed almost no clear changes over phases which agrees with Shi et al. (2021) who reported the same trend for $PM_{2.5}$ by comparing concentrations during lockdowns and before lockdown in several cities.

Fig. 7 is plotted to better address the *dw* average values during school hours. As shown in this figure, all PM followed a trend along with phases, which decreases from I to IV and then increases in phase V. For example, the average *dw* $PM_{2.5}$ concentration reduced by 22.3 %, 42.7 %, and 0.6 % from phase II to I, phase III to II, and phase IV to III, while the concentration increased by 22.7 % from phase V to IV, respectively. This is relatively similar among all size fractions of PM and is probably influenced by the same factors (see Fig. 5). The concentration of gaseous pollutants started to decrease from phase I before returning to relatively the same level in phase V. For example, the change in average *dw* NO_2 concentrations from phase I to V were −7.2, −7.1, 4.0 and 4.2 %, respectively. However, O_3 behaved oppositely to NO_2 (30.5, 20.6, −21.5, and −2.2 %, accordingly) due to an increase in the consumption rate of NO_2 in the presence of spring and

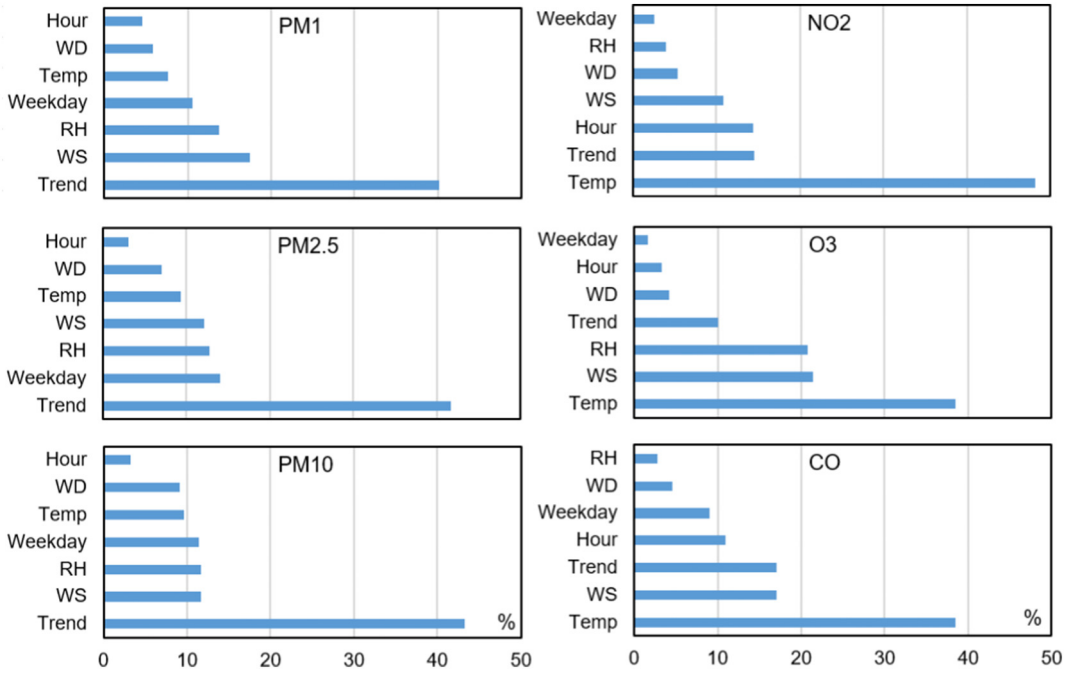

Fig. 5. The relative importance and levels of the explanatory variables for each pollutant, where their contribution in percent illustrates the relative importance and levels of the explanatory variables for that specific pollutant in the model. Importance of predictor features: the trend is time variables represented by Unix Epoch time, temperature (temp), RH, WS, WD, the hour of the day (hour), and day of the year (weekday) in the random forest model. The trend, temperature, WS and RH terms are the dominant explanatory variables throughout.

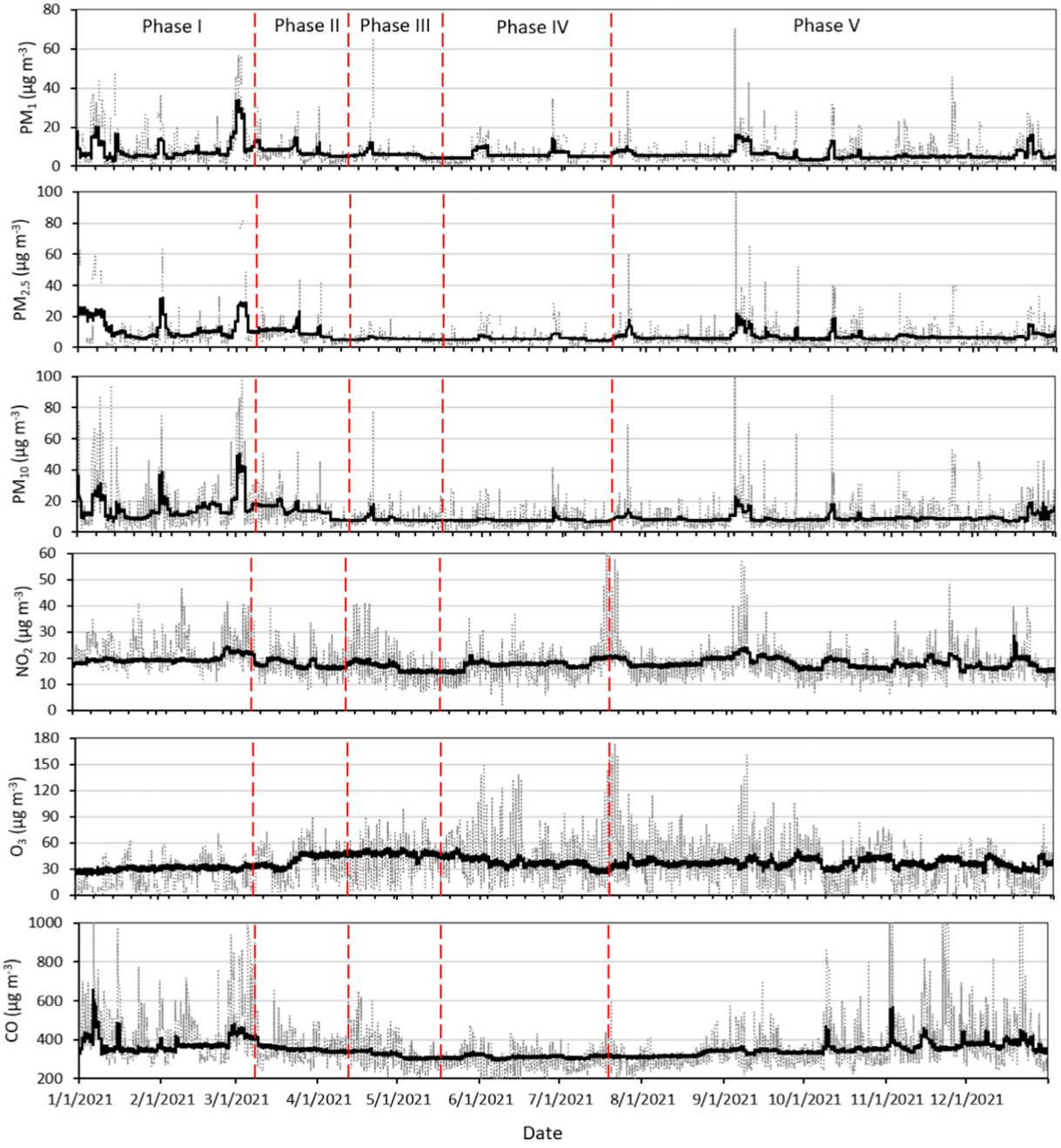

Fig. 6. Observed (dashed grey) and *dw* (solid black) hourly PM_1, $PM_{2.5}$, PM_{10}, NO_2, O_3, and CO concentrations on the school site during different phases of the study. The *dw* model was constructed with 80 % random data for training and 20 % unseen data for validation. Data is shown from January to December in 2021, where the vertical red lines separate the phases. Sample sizes for drawing the time series are 1584, 840, 840, 1512 and 2520 for phases I to V, respectively. The hourly time variation of the environmental parameters and pollution concentrations were also plotted (Fig. S3).

summer sunlight (influenced by temperature). A closer look shows that the situation is not going to be optimal for school children as concentration trends kept increasing in phase V, when the new school year started.

3.3. Forecasting model

Air pollution forecasting can be quite unpredictable, especially given the knowledge required to consider meteorological factors, emission sources, local incidents, etc., which require complex formulation with a rigorous mathematical underpinning. Here, we explored the possibility of using the Prophet algorithm to develop a forecast model for the school to take action by the cancellation of any outdoor activities. It is obvious that any forecast would be valid upon experiencing the situations it had been trained for. However, altering traffic very near to school, events such as unexpected loading or unloading, car queuing due to accidents, construction and road activities and other similar unusual occurrences could possibly slow down the flow of vehicles. In such situations, the model's accuracy will be reduced, hence, additional precautions should be taken to cancel any outdoor activities.

Here, we developed a model using a dataset covering periods of national lockdown, a series of loosening restrictions and normal situations (Fig. 8). The model captures the diurnal trends at the school site; the median points demonstrate the tendency towards over-prediction and the interquartile range represents the relatively tighter distribution of the forecasts. Although the model followed the observed NO_2 trend during January 2022, the correlation between observed and predicted values (R^2, 0.48; RMSE,

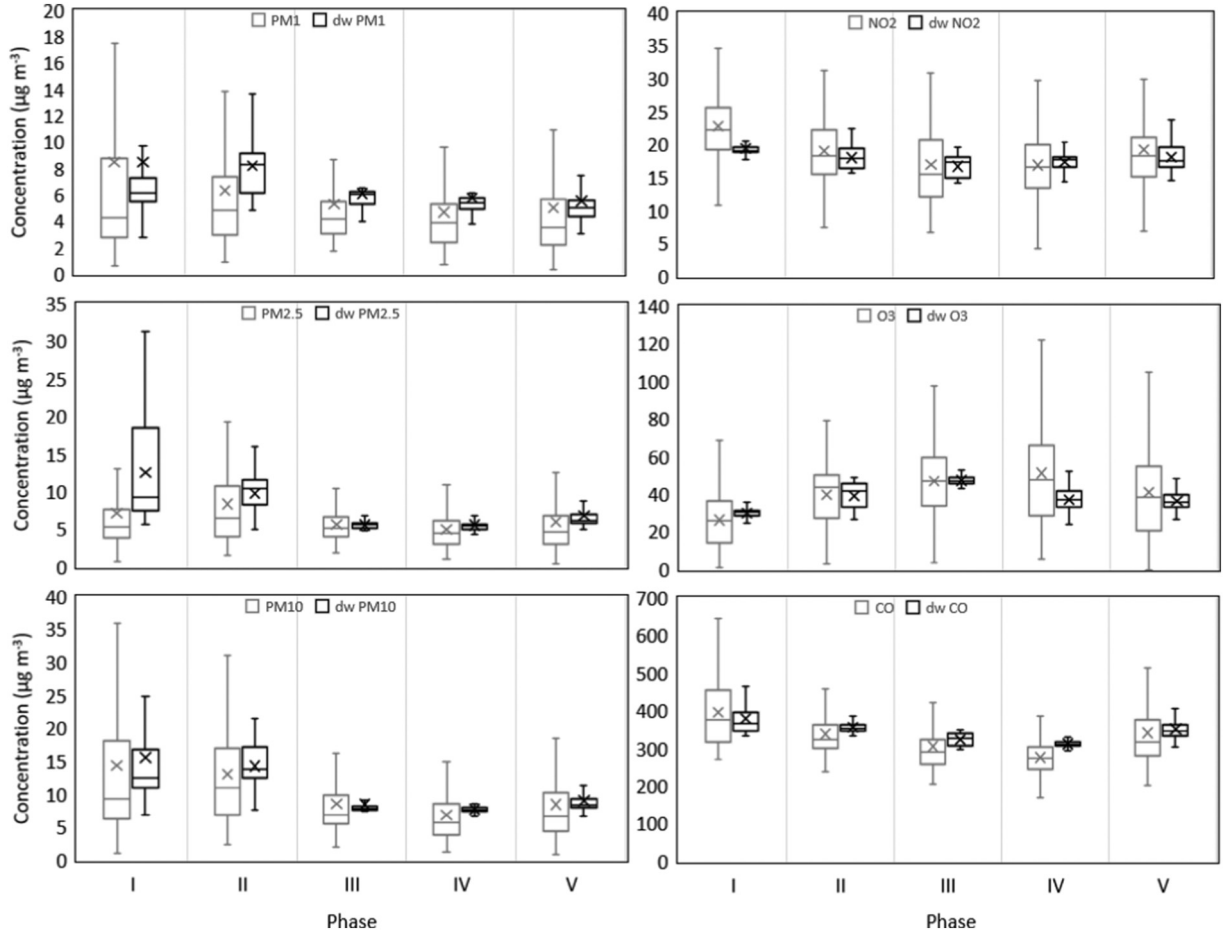

Fig. 7. Box plots of each pollutant show variations in observed and *dw* concentrations during school hours in different phases. Box plots coloured grey represent observed concentrations, while the ones in solid black represent the *dw* concentrations. Lower and upper boundaries of box plots represent the 25th and 75th percentiles, respectively; line and cross marks inside boxes represent median and average values, respectively; lower and upper error lines represent 1.5 × IQR (interquartile range) below the 3rd quartile and above the 1st quartile, respectively. The sample sizes for drawing the plots varied from 414, 225, 225, 405, and 675 for phases I to V, respectively.

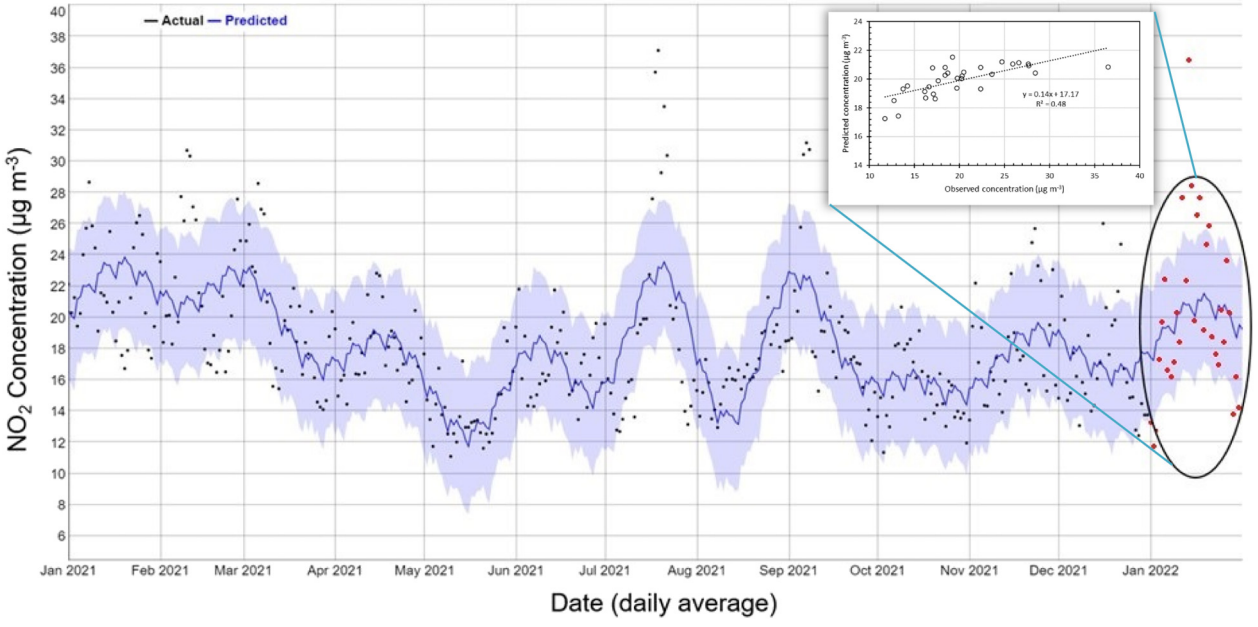

Fig. 8. Predicted (blue line) against observed NO_2 concentrations (black dots) for the entire year of 2021 at the school site. The light blue shaded area represents the uncertainty interval, which is composed of uncertainty between the trend and observation noise (Taylor and Letham, 2018).

4.7; MAE, 3.6 μg m^{-3}; Fig. 8) was found to be moderate considering the basic model inputs (date/time and NO_2 concentration) and the number of uncontrolled/changeable factors. Furthermore, the NO_2 dataset in January 2022 represents normal conditions with no lockdown in place, while the model was not trained for such conditions. Therefore, an extended dataset covering a longer period is needed to train/asses the model and devise precautionary actions.

4. Conclusions

Long-term monitoring of ambient air pollutants was carried out at the main gate of a UK primary school, which was surrounded by heavily-trafficked roads. The study was co-designed collaboratively by parents and the school to assess the impact of vehicular emissions from nearby busy roads on school children's exposure to PM_1, $PM_{2.5}$, PM_{10}, NO_2, O_3 and CO during school hours. The sampling period covered different phases, including national lockdown and different steps of loosening restrictions. To better understand the impacts of meteorological factors on the transport of air pollutants, the *dw* algorithm was applied to the dataset. Finally, the use of a simple but effective forecasting model to predict local air pollution at the school site was assessed. The following conclusions are drawn:

- New Year fireworks increased $PM_{2.5}$ concentration by up to three-times that of the WHO daily average threshold limit. Additionally, the presence of an in-school pollution source elevated daily average PM concentrations by 11–18 times with respect to the baseline concentration on previous days. Therefore, extra caution should be taken for outdoor activities in schools on the days when such events happen.
- The school children's exposure to air pollution during morning peak hours is up to 1.5-times greater as compared to daily off-peak hours. The use of vehicles should be prohibited very near to school premises (e.g. playgrounds or school entrances, such as doors/windows) to limit the build-up of local pollution levels. Also, any new school buildings should be built away from main roads.
- The level of TRAP after school reopening increased slightly, as seen by the elevated daily $PM_{2.5}$ concentrations in March compared with earlier months. After the re-opening of the school, the daily $PM_{2.5}$ level exceeded the 24-hour average (15 μg m^{-3}) limit set by the WHO on several days due to an increase in the number of on-road cars.
- High NO_2 concentrations were observed during morning peak hours. NO_2 and O_3 showed a strong reciprocal relationship during the first three phases. Elevated photochemical reactions and lifting restrictions are found to be the reasons for increased O_3 levels from mid-March onwards.
- The CO level at the school site was found to be below the DEFRA guideline. However, elevated concentrations of CO were detected, possibly due to biomass burning activities in nearby houses during cold seasons. A detailed source apportionment analysis supported by additional monitoring is required to track the CO concentrations in the school environment and apportion them to possible sources during different seasons.
- The *dw* trends revealed some variations in school hours over all phases. There were no distinguishable sharp increases or sudden decreases in *dw* time-series concentrations of pollutants from one phase to another. This confirms that the sources of the possible key pollutant emitters were present during all days and phases. However, the *dw* average values specifically during school hours revealed some slight trends, including an increasing trend from phase III/IV onwards, except for the secondary pollutant O_3. This can be a sign of a return to normal conditions after the national lockdown.
- Combustion of fossil fuels by on-road vehicles is a dominant source of NO_2 near trafficked roads. Therefore, NO_2 is a good proxy for vehicular emissions at the school sites. The Prophet model performed modestly against the observed data. However, continuous monitoring and feeding real-time concentration data into a forecasting model can improve its performance further and help schools to make evidence-based decisions ahead of time.

The study showed that schools near busy roads are more disproportionately affected by air pollution. Therefore, adopting guidelines and strategies including applying mitigation steps such as green barriers in outdoor school settings (e.g. Kumar et al., 2020a) and school streets (Abhijith et al., 2022) and toolkits for cleaner air in schools (e.g. GLA, 2018; Global Action Plan, 2020), are important measures to reduce school children's exposure to air pollution. Their adoption can be more effective when implemented through partnerships and by engaging parents and school children through citizen science initiatives such as creating their own scientific experiments and eliciting ideas on how to mitigate and improve air quality around their schools.

CRediT authorship contribution statement

Prashant Kumar: Conceptualization, Funding acquisition, Project administration, Resources, Supervision, Methodology, Formal analysis, Writing – original draft, Writing – review & editing, Visualization. **Hamid Omidvarborna:** Data curation, Methodology, Formal analysis, Writing – original draft, Writing – review & editing, Visualization. **Runming Yao:** Writing – review & editing.

Data availability

Data will be made available on request.

Declaration of competing interest

The authors declare that they have no known competing financial interests or personal relationships that could have appeared to influence the work reported in this paper.

Acknowledgement

We acknowledge the support from Innovate UK funded project 'MyGlobalHome' the pilot demonstrator under the Technology Strategy Board File Reference of 106168, the EPSRC-funded CO-TRACE (COvid-19 Transmission Risk Assessment Case studies - Education Establishments; EP/W001411/1); the INHALE (Health assessment across biological length scales for personal pollution exposure and its mitigation; EP/T003189/1); and the RECLAIM Network Plus (EP EP/W034034/1) projects, and the RealAir project in collaboration with Zero Carbon Guildford (ZERO) supported through the University of Surrey's HEIF funding. This work was a joint effort by the local community groups, the school and the researchers as a part of the GCARE's GLL initiative. We thank the school staff (Kate Collins, Tom Carroll, Neil Osmand), members of the parent group (Kate Alger, Claire Barratt, Jen Gale, Rachel Spruce, Christina Kelly, Paul Cartwright, Victoria Hazael, Bronwen Smith-Thomas, Ashley Stapledon, Melanie Hancox, Sadhana Shishodia), local councillors (Caroline Reeves, Jan Harwood, Cait Taylor), Zero Carbon Guildford (Ben McCallan) and the GCARE researchers (KV Abhijith, Yendle Barwise, Arvind Tiwari, Ana Paula Mendis Emydgio) for helping with the co-design, equipment installation and study implementation. The international collaboration with the SuDBE centre (B13041) at Chongqing University is also acknowledged.

Appendix A. Supplementary data

Supplementary data to this article can be found online at https://doi.org/10.1016/j.scitotenv.2022.160587.

References

Abhijith, K.V., Kumar, P., Gallagher, J., McNabola, A., Baldauf, R., Pilla, F., Broderick, B., Di Sabatino, S., Pulvirenti, B., 2017. Air pollution abatement performances of green infrastructure in open road and built-up street canyon environments–a review. Atmos. Environ. 162, 71–86.

Abhijith, K.V., Kumar, P., 2019. Field investigations for evaluating green infrastructure effects on air quality in open-road conditions. Atmos. Environ. 201, 132–147.

Abhijith, K.V., Kukadia, V., Kumar, P., 2022. Investigation of air pollution mitigation measures, ventilation, and indoor air quality at three schools in London. Atmos. Environ. 289, 119303.
Al-Dabbous, A.N., Kumar, P., 2014. The influence of roadside vegetation barriers on airborne nanoparticles and pedestrians exposure under varying wind conditions. Atmos. Environ. 90, 113–124.
Brumberg, H.L., Karr, C.J., Bole, A., Ahdoot, S., Balk, S.J., Bernstein, A.S., Byron, L.G., Landrigan, P.J., Marcus, S.M., Nerlinger, A.L., Pacheco, S.E., 2021. Ambient air pollution: health hazards to children. Pediatrics 147, e2021051484.
Carslaw, D.C., Ropkins, K., 2012. Openair - an R package for air quality data analysis. Environ. Model Softw. 27, 52–61.
Carslaw, D.C., Taylor, P.J., 2009. Analysis of air pollution data at a mixed source location using boosted regression trees. Atmos. Environ. 43, 3563–3570.
Carslaw, D., 2020. Deweather: an R package to remove meteorological variation from air quality data. GitHub. https://github.com/davidcarslaw/deweather. (Accessed 24 September 2021).
Castell, N., Schneider, P., Grossberndt, S., Fredriksen, M.F., Sousa-Santos, G., Vogt, M., Bartonova, A., 2018. Localized real-time information on outdoor air quality at kindergartens in Oslo, Norway using low-cost sensor nodes. Environ. Res. 165, 410–419.
CFD, 2021. Car Free Day brought Guildford Living Lab and the local community together. published online at https://www.surrey.ac.uk/news/car-free-day-brought-guildford-living-lab-and-local-community-together. (Accessed 26 June 2022).
Chen, K., Breitner, S., Wolf, K., Stafoggia, M., Sera, F., Vicedo-Cabrera, A.M., Guo, Y., Tong, S., Lavigne, E., Matus, P., Valdés, N., 2021. Ambient carbon monoxide and daily mortality: a global time-series study in 337 cities. Lancet Planet. Health 5, e191–e199.
Crilley, L.R., Shaw, M., Pound, R., Kramer, L.J., Price, R., Young, S., Lewis, A.C., Pope, F.D., 2018. Evaluation of a low-cost optical particle counter (Alphasense OPC-N2) for ambient air monitoring. Atmos. Meas. Tech. 11, 709–720.
Deters, J.K., Zalakeviciute, R., Gonzalez, M., Rybarczyk, Y., 2017. Modeling PM2.5 urban pollution using machine learning and selected meteorological parameters. J. Electr. Comput. Eng. 2017, 1–14 5106045.
DfT, 2012. Guidance on Road Classification and the Primary Route Network. https://assets.publishing.service.gov.uk/government/uploads/system/uploads/attachment_data/file/315783/road-classification-guidance.pdf. (Accessed 24 October 2022).
DfT, 2021. Official Statistics, Transport use during the coronavirus (COVID-19) pandemic. published online at https://www.gov.uk/government/statistics/transport-use-during-the-coronavirus-covid-19-pandemic. (Accessed 8 March 2021).
Dowler, C., Howard, E., 2017. More than 1,000 nurseries nationwide close to illegally polluted roads. published online at https://unearthed.greenpeace.org/2017/04/04/air-pollution-nurseries/. (Accessed 24 May 2022).
Emery, C., Liu, Z., Russell, A.G., Odman, M.T., Yarwood, G., Kumar, N., 2017. Recommendations on statistics and benchmarks to assess photochemical model performance. J. Air Waste Manage. Assoc. 67, 582–598.
Friedman, J.H., 2001. Greedy function approximation: a gradient boosting machine. Ann. Stat. 29, 1189–1232.
Fuller, G.W., Carslaw, D.C., Lodge, H.W., 2002. An empirical approach for the prediction of daily mean PM10 concentrations. Atmos. Environ. 36, 1431–1441.
Gkatzelis, G.I., Gilman, J.B., Brown, S.S., Eskes, H., Gomes, A.R., Lange, A.C., McDonald, B.C., Peischl, J., Petzold, A., Thompson, C.R., Kiendler-Scharr, A., 2021. The global impacts of COVID-19 lockdowns on urban air pollution: a critical review and recommendations. Elementa 9, 00176.
GLA, 2018. Toolkit of Measures to Improve Air Quality at Schools. published online at https://www.london.gov.uk/sites/default/files/school_aq_audits_-_toolkit_of_measures_dr_v3.3.pdf. (Accessed 3 June 2022).
GLL, 2021. Guildford Living Lab joins forces with local school to improve air quality. published online at https://www.surrey.ac.uk/news/guildford-living-lab-joins-forces-local-school-improve-air-quality. (Accessed 3 June 2022).
Global Action Plan, 2020. The clean air for schools framework. Published online at https://www.globalactionplan.org.uk/clean-air/clean-air-for-schools-framework. (Accessed 3 June 2022).
Goel, A., Kumar, P., 2016. Vertical and horizontal variability in airborne nanoparticles and their exposure around signalised traffic intersections. Environ. Pollut. 214, 54–69.
GOV.UK, 2018. Guidance, Health matters: air pollution. https://www.gov.uk/government/publications/health-matters-air-pollution/health-matters-air-pollution. (Accessed 10 June 2021).
GOV.UK, 2020. Speech: Prime Minister's statement on coronavirus (COVID-19). 23 March 2020, online at https://www.gov.uk/government/speeches/pm-address-to-the-nation-on-coronavirus-23-march-2020. (Accessed 10 June 2021).
GOV.UK, 2021. Prime Minister announces national lockdown, press release. https://www.gov.uk/government/news/prime-minister-announces-national-lockdown. (Accessed 11 June 2021) (2015).
Grange, S.K., Lee, J.D., Drysdale, W.S., Lewis, A.C., Hueglin, C., Emmenegger, L., Carslaw, D.C., 2021. COVID-19 lockdowns highlight a risk of increasing ozone pollution in European urban areas. Atmos. Chem. Phys. 21, 4169–4185.
Grange, S.K., Carslaw, D.C., 2019. Using meteorological normalisation to detect interventions in air quality time series. Sci. Total Environ. 653, 578–588.
Henneman, L.R., Liu, C., Hu, Y., Mulholland, J.A., Russell, A.G., 2017. Air quality modeling for accountability research: operational, dynamic, and diagnostic evaluation. Atmos. Environ. 166, 551–565.
Hickman, A.L., Baker, C.J., Cai, X., Delgado-Saborit, J.M., Thornes, J.E., 2018. Evaluation of air quality at the Birmingham New Street Railway Station. Proc. Inst. Mech. Eng. F J. Rail Rapid Transit 232, 1864–1878.
Jayaratne, R., Liu, X., Thai, P., Dunbabin, M., Morawska, L., 2018. The influence of humidity on the performance of a low-cost air particle mass sensor and the effect of atmospheric fog. Atmos.Meas.Tech. 11, 4883–4890.
Kakoullis, L., Eliades, E., Papachristodoulou, E., Parperis, K., Chra, P., Constantinidou, A., Chatzittofis, A., Sampsonas, F., Panos, G., 2021. Response to COVID-19 in Cyprus: policy changes and epidemic trends. Int. J. Clin. Pract. 75, e13944.
Kumar, P., Morawska, L., Martani, C., Biskos, G., Neophytou, M., Di Sabatino, S., Bell, M., Norford, L., Britter, R., 2015. The rise of low-cost sensing for managing air pollution in cities. Environ. Int. 75, 199–205.
Kumar, P., Omidvarborna, H., Barwise, Y., Tiwari, A., 2020a. Mitigating exposure to traffic pollution in and around schools: guidance for children, schools and local communities, p. 24 https://doi.org/10.5281/zenodo.3754131.
Kumar, P., Omidvarborna, H., Pilla, F., Lewin, N., 2020b. A primary school driven initiative to influence commuting style for dropping-off and picking-up of pupils. Sci. Total Environ. 727, 138360.
Kumar, P., Hama, S., Omidvarborna, H., Sharma, A., Sahani, J., Abhijith, K.V., Debele, S.E., Zavala-Reyes, J.C., Barwise, Y., Tiwari, A., 2020c. Temporary reduction in fine particulate matter due to 'anthropogenic emissions switch-off' during COVID-19 lockdown in Indian cities. Sustain. Cities Soc. 62, 102382.
Kumar, P., Omidvarborna, H., Tiwari, A., Morawska, L., 2021. The nexus between in-car aerosol concentrations, ventilation and the risk of respiratory infection. Environ. Int. 157, 106814.
Kumar, P., Omidvarborna, H., Valappil, A.K., Bristow, A., 2022. Noise and air pollution during COVID-19 lockdown easing around a school site. J. Acoust. Soc. Am. 151, 881–887.
Lee, J.D., Drysdale, W.S., Finch, D.P., Wilde, S.E., Palmer, P.I., 2020. UK surface NO2 levels dropped by 42% during the COVID-19 lockdown: impact on surface O3. Atmos. Chem. Phys. 20, 15743–15759.
Li, Y., Chen, Q., Zhao, H., Wang, L., Tao, R., 2015. Variations in PM10, PM2.5 and PM1.0 in an urban area of the Sichuan Basin and their relation to meteorological factors. Atmosphere 6, 150–163.
Mahajan, S., Kumar, P., 2019. Sense Your Data: Sensor Toolbox Manual, Version 1.0, pp. 1–7 https://doi.org/10.13140/RG.2.2.17249.76640/4.
Mahajan, S., Kumar, P., Antonino Pinto, J., Riccetti, A., Schaaf, K., Camprodon, G., Smári, V., Passani, A., Forino, G., 2020. A citizen science approach for enhancing public understanding of air pollution. Sustain. Cities Soc. 52, 101800.
Mahato, S., Pal, S., Ghosh, K.G., 2020. Effect of lockdown amid COVID-19 pandemic on air quality of the megacity Delhi,India. Sci. Total Environ. 730, 139086.
Monks, P.S., Archibald, A.T., Colette, A., Cooper, O., Coyle, M., Derwent, R., Fowler, D., Granier, C., Law, K.S., Mills, G.E., Stevenson, D.S., 2015. Tropospheric ozone and its precursors from the urban to the global scale from air quality to short-lived climate forcer. Atmos. Chem. Phys. 15, 8889–8973.
NAEI, 2021. Overview of Air Pollutants. National Atmospheric Emissions Inventory, UK https://naei.beis.gov.uk/overview/ap-overview (accessed 22 September 2021).
Nath, P., Saha, P., Middya, A.I., Roy, S., 2021. Long-term time-series pollution forecast using statistical and deep learning methods. Neural Comput. Applic. 1–20.
Office for National Statistics, 2021. How the population changed in Guildford: Census 2021. published online at https://www.ons.gov.uk/visualisations/censuspopulationchange/E07000209/. (Accessed 24 October 2022).
Omidvarborna, H., Kumar, P., Tiwari, A., 2020. 'Envilution™' chamber for performance evaluation of low-cost sensors. Atmos. Environ. 223, 117264.
Omidvarborna, H., Kumar, P., Hayward, J., Gupta, M., Nascimento, E.G.S., 2021. Low-cost air quality sensing towards smart homes. Atmosphere 12, 453.
Osborne, S., Uche, O., Mitsakou, C., Exley, K., Dimitroulopoulou, S., 2021a. Air quality around schools: part I-A comprehensive literature review across high-income countries. Environ. Res. 196, 110817.
Osborne, S., Uche, O., Mitsakou, C., Exley, K., Dimitroulopoulou, S., 2021b. Air quality around schools: part II-mapping PM2.5 concentrations and inequality analysis. Environ. Res. 197, 111038.
Perscom, 2018. National Travel Survey. https://www.gov.uk/government/statistical-data-sets/nts06-age-gender-and-modal-breakdown. (Accessed 10 June 2021).
PHE, 2020. The Health Protection (Coronavirus, Restrictions) (England) Regulations 2020 (and associated amendments). online at http://www.legislation.gov.uk/uksi/2020/350/pdfs/uksi_20200350_en.pdf. (Accessed 10 June 2021).
R Development Core Team, 2013. R: A Language And Environment for Statistical Computing, pp. 1–16.
Ragettli, M.S., Phuleria, H.C., Tsai, M.Y., Schindler, C., De Nazelle, A., Ducret-Stich, R.E., Ineichen, A., Perez, L., Braun-Fahrländer, C., Probst-Hensch, N., Künzli, N., 2015. The relevance of commuter and work/school exposure in an epidemiological study on traffic-related air pollution. J. Expo. Sci. Environ. Epidemiol. 25, 474–481.
Rai, A.C., Kumar, P., Pilla, F., Skouloudis, A.N., Di Sabatino, S., Ratti, C., Yasar, A., Rickerby, D., 2017. End-user perspective of low-cost sensors for outdoor air pollution monitoring. Sci. Total Environ. 607, 691–705.
Sadhasivam, J., Muthukumaran, V., Raja, J.T., Vinothkumar, V., Deepa, R., Nivedita, V., 2021. Applying data mining technique to predict trends in air pollution in Mumbai. JulyJournal of Physics: Conference Series. Vol. 1964. IOP Publishing, p. 042055 No. 4.
Samal, K.K.R., Babu, K.S., Das, S.K., Acharaya, A., 2019. Time Series based air pollution forecasting using SARIMA and Prophet model. AugustProceedings of the 2019 International Conference on Information Technology And Computer Communications, pp. 80–85.
Sharma, A., Kumar, P., 2018. A review of factors surrounding the air pollution exposure to in-pram babies and mitigation strategies. Environ. Int. 120, 262–278.
Shi, Z., Song, C., Liu, B., Lu, G., Xu, J., Van Vu, T., Elliott, R.J., Li, W., Bloss, W.J., Harrison, R.M., 2021. Abrupt but smaller than expected changes in surface air quality attributable to COVID-19 lockdowns. Sci. Adv. 7, eabd6696.
Shier, V., Nicosia, N., Shih, R., Datar, A., 2019. Ambient air pollution and children's cognitive outcomes. Popul. Environ. 40, 347–367.
Surrey-i, 2015. Census Key Statistics (Key Demographics, Age, Gender, Ethnicity, Religion, Disability, Health And Carers). Guildford Local Authority in Surrey, pp. 25–27.
Taylor, S.J., Letham, B., 2018. Forecasting at scale. Am. Stat. 72, 37–45.

Tiwari, A., Kumar, P., Kalaiarasan, G., Ottosen, T.B., 2021. The impacts of existing and hypothetical green infrastructure scenarios on urban heat island formation. Environ. Pollut. 274, 115898.

Topping, D., Watts, D., Coe, H., Evans, J., Bannan, T.J., Lowe, D., Jay, C., Taylor, J.W., 2020. Evaluating the use of Facebook's Prophet model v0.6 in forecasting concentrations of NO2 at single sites across the UK and in response to the COVID-19 lockdown in Manchester, England. Geoscientific Model Development Discussions, pp. 1–22.

UK Air, 2021. What is the Daily Air Quality Index? https://uk-air.defra.gov.uk/air-pollution/daqi?view=more-info&pollutant=pm25. (Accessed 20 November 2021) License: CC BY-NC-SA 3.0 IGO

Venter, Z.S., Aunan, K., Chowdhury, S., Lelieveld, J., 2020. COVID-19 lockdowns cause global air pollution declines. Proc. Natl. Acad. Sci. 117, 18984–18990.

World Health Organization, 2021. WHO global air quality guidelines: particulate matter (PM2.5 and PM10), ozone, nitrogen dioxide, sulfur dioxide and carbon monoxide. World Health Organization License: CC BY-NC-SA 3.0 IGO https://apps.who.int/iris/handle/10665/345329.

Xi, X., Wei, Z., Xiaoguang, R., Yijie, W., Xinxin, B., Wenjun, Y., Jin, D., 2015. A comprehensive evaluation of air pollution prediction improvement by a machine learning method. 2015 IEEE International Conference on Service Operations and Logistics, and Informatics (SOLI), pp. 176–181 https://naei.beis.gov.uk/overview/ap-overview (accessed 22 September 2021).

Ye, Z., 2019. Air pollutants prediction in Shenzhen based on ARIMA and Prophet method. E3S Web of ConferencesVol. 136. EDP Sciences, p. 05001.